

Lattice modes in ferroelectric perovskites. II. $\text{Pb}_{1-x}\text{Ba}_x\text{TiO}_3$ including BaTiO_3 [†]

Gerald Burns

IBM Thomas J. Watson Research Center, Yorktown Heights, New York 10598

(Received 6 March 1974)

The Raman measurements of the ferroelectric PbTiO_3 reported previously are extended to the ferroelectric system $(\text{Pb}_{1-x}\text{Ba}_x)\text{TiO}_3$ including the end member BaTiO_3 . The measurements were made on crystals of BaTiO_3 , very small crystals for several x , and powders using the powder Raman technique. The expected $3n-3$ optic modes are accounted for at all x including BaTiO_3 . These modes in BaTiO_3 obey the proper selection rules and disappear and reappear abruptly at the transition temperature T_c when approached from below or above, respectively. This is contrary to what is often suggested in the literature. Of course there are other broad bands observed in BaTiO_3 that do not disappear at T_c . These broad bands are only found for $x \approx 0.9$ to 1. Similarly, the room-temperature data show that the lowest soft $E(\text{TO})$ mode is overdamped only for $x \approx 0.9$ to 1. For smaller x it is underdamped at room temperature. However, the linewidth of the underdamped soft $E(\text{TO})$ mode behaves in a singular manner as T_c is approached from below as is found in PbTiO_3 . For $x = 0.9$ and 1 this singular behavior is not observed. The data on the soft $E(\text{TO})$ mode in BaTiO_3 show that the shape of the response is practically independent of temperature in agreement with earlier work. Also, the intensity is practically independent of temperature in strong disagreement with earlier work. We cannot unambiguously determine the undamped frequency and linewidth of this mode, and we feel that the temperature dependences of these quantities, for the soft $E(\text{TO})$ mode in BaTiO_3 , are not as yet determined. The frequency of the modes is a fairly continuous function of x even though there are several phase transitions on the BaTiO_3 -rich end. Lastly, some discussion of the temperature dependence of the dielectric constant in terms of impurities and the concept of dirty displacive ferroelectrics is given. Very large enhancements of the static dielectric constant can be obtained due to interaction with the soft modes.

I. INTRODUCTION

In this paper we continue the work of an earlier paper¹ (henceforth called I) which describes the lattice normal modes in the ferroelectric phase of PbTiO_3 . These modes were measured by the Raman technique below the ferroelectric transition temperature² T_c . There has been relatively little work on the modes in the ferroelectric phase of simple materials like the perovskites ABO_3 . The original ideas³ exploring the origin of ferroelectricity via a lattice-mode instability emphasized the high-temperature paraelectric phase. In I we showed that PbTiO_3 is a "textbook" example of a ferroelectric below T_c with respect to the lattice modes. That is, the modes obey the appropriate Raman selection rules; the modes are underdamped up to T_c (although the soft-mode damping has an interesting temperature dependence); the lines disappear abruptly at T_c when the crystal becomes centrosymmetric, as they should. It was also shown that there is very poor agreement between the simple Devonshire theory² and dielectric properties that could be determined from the modes.

In this paper the temperature dependence of the modes in the solid solution $\text{Pb}_{1-x}\text{Ba}_x\text{TiO}_3$ is investigated. This includes $x=1$, or BaTiO_3 , which is the classic ferroelectric perovskite crystal. It will be shown that the modes behave in a continuous manner as a function of x . However, they

behave quite differently on the BaTiO_3 -rich side than for $x=0$. Nevertheless, the $3n-3$ optic modes obey the appropriate selection rules and could be measured right up to T_c for BaTiO_3 , at which temperature they also abruptly disappear, as they should. This is contrary to what is often stated or assumed in the literature. Of course, the broad, apparently second-order modes do not disappear at T_c . Thus, when the correct modes are observed in BaTiO_3 they also behave as expected, except that one of the modes is overdamped.⁴⁻⁷

The type of samples used here differ from those used in I. In I only single crystals were used. Here we used a large single crystal ($3 \times 3 \times 3$ mm) of BaTiO_3 as well as a good-quality butterfly crystal; however, for $0 \leq x \leq 1$ we have exploited the powder Raman technique⁸ as well as small imperfect crystals.

Since BaTiO_3 is the classic ferroelectric perovskite material, one might think that the vibrational modes are well understood and the temperature dependence known. Actually this is not true, partly because there is some strong second-order Raman scattering that has been interpreted as first-order spectra and because one of the modes is overdamped. The early^{9,10} single-domain Raman measurements on BaTiO_3 were substantially in agreement with each other. However, these papers did not

agree with each other or with the infrared work⁴⁻⁶ on the lowest E mode. Later Raman work⁷ showed an overdamped E mode in agreement with the infrared measurements. Still later Raman work¹¹ yielded E modes in agreement with the earlier measurements but yielded transverse A_1 modes in disagreement with the work in Refs. 9 and 10. Since the A_1 modes were not measured by infrared techniques, no comparison could be made there. Polariton measurements at room temperature¹² have cleared up the A_1 -modes disagreement. The results are in agreement with the early Raman work^{9,10} and in disagreement with the more recent work.¹¹ The room-temperature polariton work¹² has been checked by a different approach. Using the powder Raman technique,⁸ results for BaTiO_3 at room temperature have been found by an extension of measurements¹³ on $\text{Pb}_{1-x}\text{Ba}_x\text{TiO}_3$. These results are in excellent agreement with the room-temperature polariton results.¹² The temperature dependence of the A_1 modes now has been measured¹⁴ using the polariton technique. An interesting aspect of these results will be discussed later.

II. EXPERIMENTAL

The Raman measurements were carried out as described in I. A He-Ne laser was used for the powder Raman measurements and an argon laser (5145 Å, 300×10^{-3} W) was used on the single crystals. The furnace was described in I.

A large BaTiO_3 single crystal was obtained from Sanders. The transition temperature is 134°C with increasing temperature. We also measured one "butterfly" grown by the Remeika method.¹⁵ The results from the two crystals were the same except that $T_c = 120^\circ\text{C}$ for the butterfly BaTiO_3 .

The powder Raman technique was applied to sintered pellets of $\text{Pb}_{1-x}\text{Ba}_x\text{TiO}_3$ prepared by first reacting PbTiO_3 - BaTiO_3 mixtures with various values of x at 800°C for 16 h. Subsequently, approximately 2-g pellets of each sample were sintered twice at temperatures between 1000 and 1200°C for 2 h with an intermediate grinding and pressing step. Each sample was contained in a platinum "pillbox," and this was, in turn, surrounded by $\text{Pb}_{1-x}\text{Ba}_x\text{TiO}_3$ powder of identical composition within a covered 25-cm³ platinum crucible. The resulting $\text{Pb}_{1-x}\text{Ba}_x\text{TiO}_3$ samples were examined by Grunier x-ray diffraction techniques, and a lattice-constant-vs- x diagram was constructed. These data are shown in Fig. 1, where they are compared with the early published work.¹⁶ The agreement between the present results and the early work¹⁶ is fairly good. A loss of Pb during firing of this early work could account for some of the difference. Our end-member results are

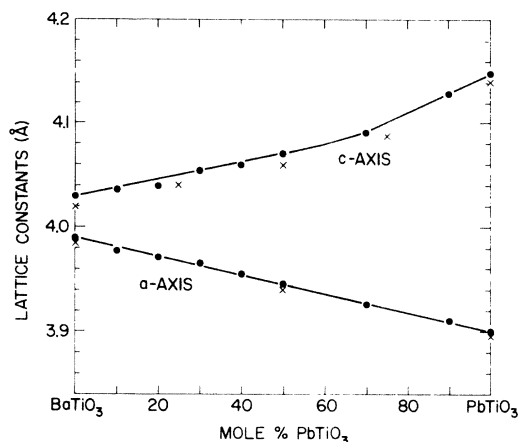


FIG. 1. Lattice constant vs composition measured on the ceramic samples as described in the text. The solid circles are data obtained here, the crosses are from Ref. 16.

in very good agreement with published results for BaTiO_3 ¹⁷ and PbTiO_3 .¹⁸

Single crystals of the solid solutions of sizes typically less than 1 mm³ were grown in the $\text{PbO-BaO-TiO}_2\text{-B}_2\text{O}_3$ system at $\text{PbO}:\text{BaO}:\text{TiO}_2:\text{B}_2\text{O}_3$ ratios in the ranges (50-70):(5-10):(10-25):(10-30). These were obtained by slowly cooling the melts from 1300°C to $\sim 900^\circ\text{C}$ in 100-cm³ covered platinum crucibles at rates between 2 and 5°C/h , and decanting the fluxed solutions at the lower temperature. Crystals were cooled to room temperature under fiberfrax insulation to minimize cracking at the phase-transition temperatures. The crystals were analyzed by electron microprobe analysis and powder x-ray diffraction to determine the precise value of x by comparison with Fig. 1. The agreement with the x value obtained via Fig. 1 and those obtained by comparing the Raman results for these small single crystals with the powder Raman results was excellent.

Polarized Raman measurements were performed on these small poor-quality single crystals. The procedure was quite simple. Various arrangements of polarizers and analyzers were tried with a given direction for a crystal. Often one set of lines would become much more intense than the rest of the lines. If, from the powder Raman results as a function of x , it is known that one of these lines transforms as, for example, the E -ir-reducible representation, then all of the lines transform likewise. Usually the other appropriate orientation of polarizers and analyzers would increase the intensity of the A_1 lines. The agreement with what was expected from the powder Raman measurements as a function of x was excellent.

III. MODES

A classification of the modes is covered in I but briefly outlined here for completeness. In the cubic phase of an ABO_3 perovskite, there are $3n - 3 = 12$ optic modes. These modes transform as the $3T_{1u} + T_{2u}$ irreducible representations of the O_h point group. The T_{2u} mode is called the "silent" mode because it is not Raman or infrared active. In the tetragonal ferroelectric phase, the point group of the crystal is C_{4v} , so the normal modes are classified according to the irreducible representations of this point group. Each of the T_{1u} modes splits into $A_1 + E$ modes in C_{4v} . Depending on the direction of propagation of the mode with respect to its polarization (mechanical separation of charge), the modes can be longitudinal optic (LO) or transverse optic (TO). So, in C_{4v} the modes that originate from the T_{1u} modes are called $A_1(\text{TO})$, $A_1(\text{LO})$, $E(\text{TO})$, or $E(\text{LO})$. In Ref. 1 we have further labeled these modes with an index 1, 2, or 3 from each of the three T_{1u} modes. However, here this extra label is not used.

The silent T_{2u} is treated slightly differently. In C_{4v} it will become $B_1 + E$, and these modes are no longer silent. Both B_1 and E modes are Raman active, and the E mode is also infrared active. In principle the E mode coming from the T_{2u} mode has a TO and LO splitting. However, in practice¹ it is too small to measure, and the separation between the B_1 and E modes cannot be measured.¹ So we keep the word *silent* as a convenient label of these modes, even in the C_{4v} phase.

The lowest $E(\text{TO})$ and $A_1(\text{TO})$ modes in the C_{4v} phase are called "soft" modes, as is customary in the field of ferroelectricity. More will be said about this soft E mode.

BaTiO_3 has other low-temperature phases² which extend^{16,19} to $x \geq 0.9$ or perhaps to slightly small x , as will be discussed. The modes in these various phases should be classified according to the appropriate point group.

IV. RESULTS FOR $0 < x < 1$

A. General temperature results

Figure 2 shows the experimental powder Raman results for $\text{Pb}_{1-x}\text{Ba}_x\text{TiO}_3$ at low temperatures. These results are analogous to those published at room temperature.¹³ Figure 3 shows the same results plotted as energy vs x . Figure 4 shows energy vs x for room-temperature data similar to those published previously, except single-crystal results are included as triangles. As can be seen, the single-crystal and powder data agree very well.

From the low-temperature results (Figs. 2 and 3) several points can be made. First, as x increases from 0 to 1, the modes above 300 cm^{-1}

vary in a fairly continuous manner. This is slightly surprising since the ferroelectric phase diagram shows that at this low temperature the $x = 0.9$ and 1.0 material is in a rhombohedral phase, while for smaller x the material is in a tetragonal phase. Actually, from a careful look at the data in Figs. 2 and 3, the change of structure might occur at $x = 0.8$. The modes at ≈ 490 and 520 cm^{-1} give very similar powder Raman spectra to each other and slightly sharper than the same modes for $x \leq 0.7$. Nevertheless, the restoring forces for these particular modes vary smoothly with x even though there is a structural phase change. So, even though the modes are labeled according to the irreducible representations of the point group C_{4v} for $x < 0.8$ and according to the irreducible representations of C_{3v} for higher x , the restoring forces for the higher-energy modes vary in a manner that effectively appears to be continuous with x . The situation for the low-energy

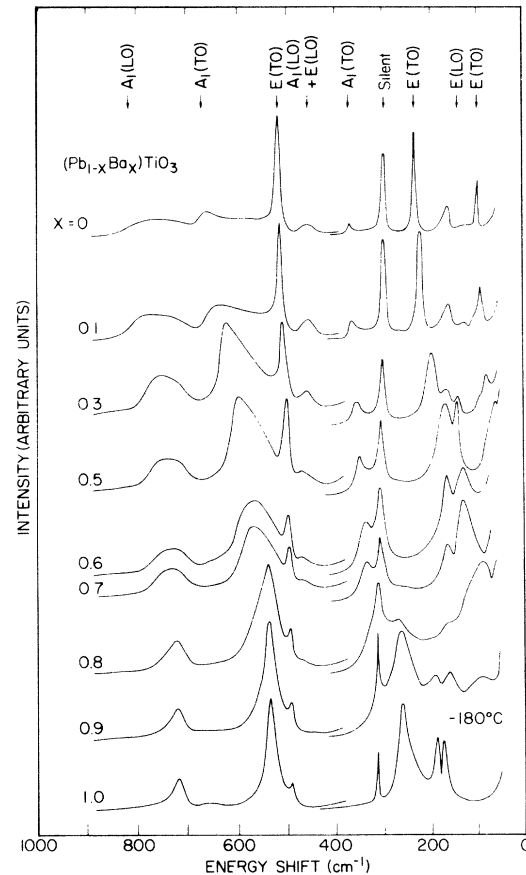


FIG. 2. Powder Raman experimental results for various x in $\text{Pb}_{1-x}\text{Ba}_x\text{TiO}_3$ at 180°C . The curves are broken at $\approx 400 \text{ cm}^{-1}$ because of a gain change. The arrows on the top are the results for various modes, as indicated, in PbTiO_3 .

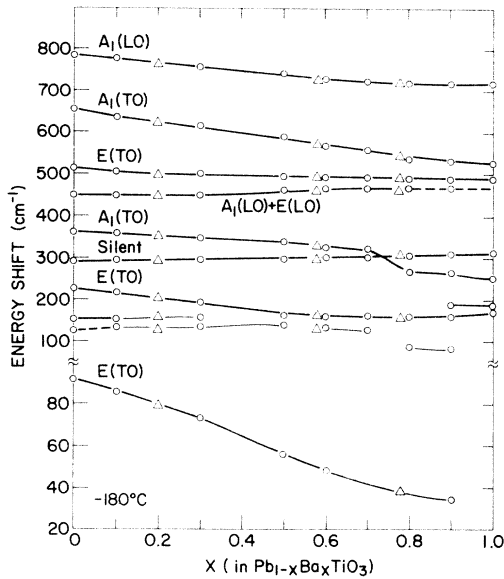


FIG. 3. Vibrational mode energies vs x are the circles from the experimental powder Raman results shown in Fig. 2. The triangles are from small single crystals as described in the text. The labels on the left refer to results in single crystals of PbTiO_3 . The unlabeled lines between 150 cm^{-1} and 100 cm^{-1} are probably due to second-order effects (Ref. 1) and purity-induced resonance modes (Ref. 23), respectively. Similar structure is shown in Fig. 4.

modes is less clear since several modes cannot be observed by the powder Raman technique even in PbTiO_3 , as can be seen in Fig. 2. These modes are very weak¹ even in single-crystal PbTiO_3 , so they are not expected to be observed in the powder Raman spectra. For example, the lowest $A_1(\text{TO})$ mode is not directly observable in¹ PbTiO_3 . Also, it is very weak in BaTiO_3 but observable at $\approx 170 \text{ cm}^{-1}$ in right-angle Raman scattering⁹⁻¹¹ and more easily seen by polariton scattering.^{12,14}

B. Soft $E(\text{TO})$ mode

The second observation from Fig. 3 is that the lowest $E(\text{TO})$ mode can be observed and is underdamped from $0 \leq x \leq 0.9$. This mode can be seen in Fig. 2 but normally is observed with much-reduced slit width in the monochromator. Even at room temperature, we have been able to observe this underdamped mode to $x=0.8$. (Reference 13 shows data to $x=0.7$, but it has been possible to extend the observation to $x=0.8$, as noted in Fig. 4.) So the fact that the lowest $E(\text{TO})$ mode in BaTiO_3 is overdamped at temperatures far from T_c is peculiar to that material, and for $x \approx 10\%$ smaller than 1 the mode is no longer overdamped.

Finally, Fig. 4 shows that agreement between

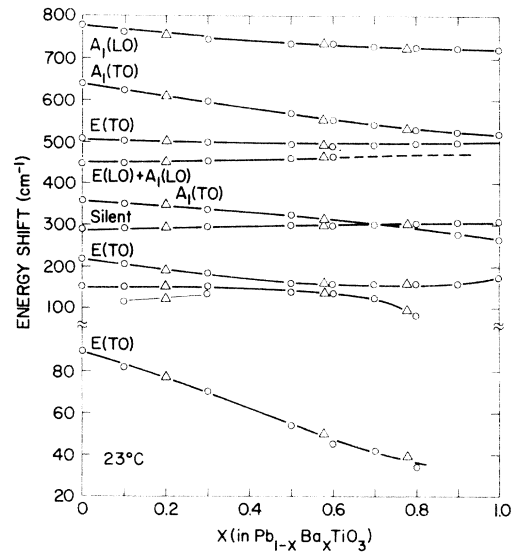


FIG. 4. Results are the same as in Fig. 3 but measured at 23°C .

the powder Raman results and the small single crystals is excellent.

Figure 5 shows the energy of the soft $E(\text{TO})$ mode for various x plotted on a reduced temperature scale. Single-crystal data for $x=0.0, 0.2, 0.58,$ and 0.78 are used as well as the data from the powder Raman method. As can be seen, only for $x=0$ and 0.2 could reliable data be obtained right up to T_c . For the single crystals $x=0.58$ and 0.78 , the damping becomes too large near T_c and

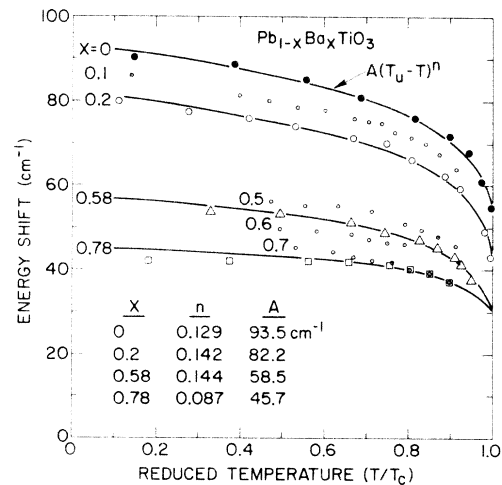


FIG. 5. Energy of the lowest $E(\text{TO})$ mode vs T/T_c from the powder Raman data for $x=0.1, 0.5, 0.6,$ and 0.7 . Small single crystals were used for the $x=0.2, 0.58,$ and 0.78 data. The lines are obtained by fitting the data as described in the text.

the crystals are of too poor quality to measure the mode properly. The large damping will be discussed later. Figure 5 also shows that the temperature dependence of the powder Raman data is in good agreement with the single crystals. However, in most cases reliable data on the powders could not be obtained at temperatures as high as on the single crystals. This was because the powder Raman data showed an anomalously large temperature-dependent linewidth near T_c . We do not understand the reason for this. Several attempts to see if it was related to particle size were inconclusive.

The solid lines in Fig. 5 are curves drawn to an extrapolation formula¹

$$\omega_{E(\text{TO})} = A \left(\frac{T_u}{T_c} - \frac{T}{T_c} \right)^n, \quad (1)$$

where A and n are chosen to fit the data over a range of T/T_c from about 0.3 to 0.9. The meaning of T_u is clearly discussed in I. It is the theoretically extrapolated temperature at which the dielectric constant in the ferroelectric phase would go to infinity if the first-order phase transition did not occur. T_u is given in terms of the transition temperature and Curie temperature T_c and T_0 , respectively:

$$T_u = T_0 + \frac{4}{3}(T_c - T_0). \quad (2)$$

To obtain T_u as a function of x , we assumed a linear variation of $T_c - T_0 = 43^\circ\text{K}$ and 11°K for $x=0$ (Ref. 20) and $x=1.0$,²¹ respectively. The resulting values of n and A (in units of $1/\text{cm}^{-1}$) are listed in Fig. 5. All of the temperature dependence of the mode frequency comes from n , as can be seen in Eq. (1). The small value of n for $x=0.78$ results from the data showing a fairly flat temperature dependence. For this value of x , the lower temperature data can be fit better with $n=0.057$. Thus, extrapolation to BaTiO_3 would result in an even smaller value of n and a very weak temperature dependence. This extrapolated result is in agreement with what we find in single-crystal BaTiO_3 , discussed later, but in disagreement with others.¹¹

C. Linewidth of the soft $E(\text{TO})$ mode

The signal to noise in the data that we could obtain from the small crystals of $x=0.58$ and 0.78 was almost as good as observed in I for PbTiO_3 . Thus, as in I, we could fit the line shape over most of the temperature range to a simple damped harmonic oscillator. [The form taken is $\epsilon(\omega) - \epsilon_\infty \propto (\omega_{\text{TO}}^2 - \omega^2 + i\gamma\omega)^{-1}$, which is slightly different from the definition of γ in Ref. 11.] However, once the mode became overdamped, we could no longer obtain ω_{TO} and γ , the damping constant, so the result could not be determined to $T/T_c=1$. Figure 6 shows the results. On this scale, γ of the soft

$E(\text{TO})$ mode in BaTiO_3 is between⁷ 70 and 90 cm^{-1} . Thus, as in¹ PbTiO_3 , it appears that the linewidth diverges as T_c is approached from below for $0 \leq x \leq 0.78$. As discussed later, this does not appear to happen for $x=1$, BaTiO_3 . The present ideas of Silverman²² concerning the divergence of the linewidth as T_c is approached could account for these data. For such crystals the divergence of the linewidth of the soft $E(\text{TO})$ phonon is caused²² by the enhancement of the scattering processes of this mode that are allowed by the finite lifetime of the phonon in the acoustic branch. The temperature variation of the energy of the $E(\text{TO})$ mode can result in a closer tuning to the frequency separation of the acoustic branches. However, for $x \approx 1$, BaTiO_3 , all these relaxation processes occur, as evidenced by the large value of the damping, so no new ones become important as the temperature is varied to T_c .

We should point out that a different type of line shape as well as temperature dependence is observed in single crystals in the low-temperature ferroelectric $(\text{K, Na})\text{TaO}_3$ system.²³

D. Low-temperature phases for $x \approx 1$

BaTiO_3 has a series of phase transitions as the temperature is lowered.² These phases are cubic (C), tetragonal (T), orthorhombic (O), and rhombohedral (R). For $x=0.9$ and 1, the phase transition between these phases occurs at¹⁶

x	$C-T$	$T-O$	$O-R$
1	120°C	5°C	-75°C
0.9	180°C	-80°C	-150°C

In order to investigate these low-temperature phases, we took the data shown in Fig. 7. It should be pointed out that several early unpolarized Raman measurements on BaTiO_3 have been

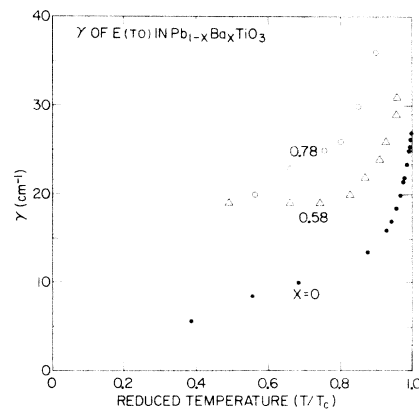


FIG. 6. The damping constant γ vs T/T_c for several x from small single crystals.

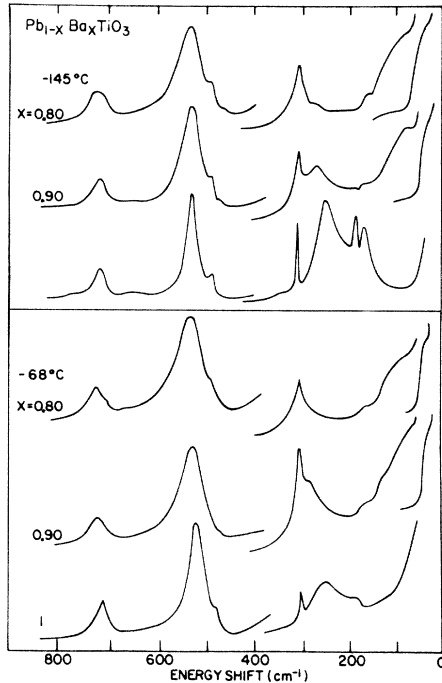


FIG. 7. Low-temperature powder Raman results for several x showing results in the low-temperature BaTiO_3 phases.

published.²⁴⁻²⁶ The unpolarized single-crystal BaTiO_3 data of Perry and Hall²⁶ are particularly interesting since they look exactly like the powder Raman results shown in Fig. 2 for BaTiO_3 . This, perhaps, is to be expected since their single-crystal work was done on a multidomain sample excited with mercury light from all directions. Relatively little was found from the high-temperature modes to identify the phase transitions. Figure 7 also shows that relatively little happens to the high-frequency modes as phase boundaries are crossed as a function of composition. The result for $x=1$ at -68°C looks similar in many respects to that for $x=0.9$ at -145°C . In both these cases the material is in the orthorhombic phase. Also, the $x=0.9$ at -180°C in Fig. 2 looks like the $x=1$ at -145°C in Fig. 7. In both of these cases the material is in the rhombohedral phase. So it is possible that the modes near the low-temperature phase transitions could be studied, but closer intervals of x and temperature would be required.

V. RESULTS FOR $x=1$ (BaTiO_3)

We would now like to consider the results for $x=1$, or BaTiO_3 . The A_1 modes that give rise to the dielectric constant along the ferroelectric z axis have been measured up to T_c and discussed

elsewhere.¹⁴ Thus, we will discuss primarily the soft $E(\text{TO})$ mode. Although in the original Raman literature there was disagreement^{9,10} about this lowest $E(\text{TO})$ mode, it is now clear from the Raman measurements that this mode is overdamped.⁷ This is in agreement with the earlier room-temperature infrared results.⁴⁻⁶

Figure 8 shows some of our experimental results on this soft $E(\text{TO})$ mode. As can be seen, we obtain an overdamped mode in agreement with DiDomenico *et al.*⁷ However, we get a different temperature dependence of the intensity. Also, by fitting the mode at different temperatures, we cannot extract a temperature dependence of the frequency with any certainty. We discuss these two points separately. Our results on the Sanders and butterfly crystals are the same.

First consider the line shape of the $E(\text{TO})$ mode. Figure 9 shows a schematic line for various values of γ/ω_0 from 0.2 to $2\sqrt{2}$. For $\gamma/\omega_0 = \sqrt{2}$ the peak of the Raman intensity occurs at $\omega = 0$. This result persists for $\gamma/\omega_0 > \sqrt{2}$. The experimental result in Fig. 8 clearly falls in this regime. We attempted to fit the shape of the experimental data by varying γ and ω_0 . The formulas¹¹ are in Fig. 9. We normalized the experimental and calcu-

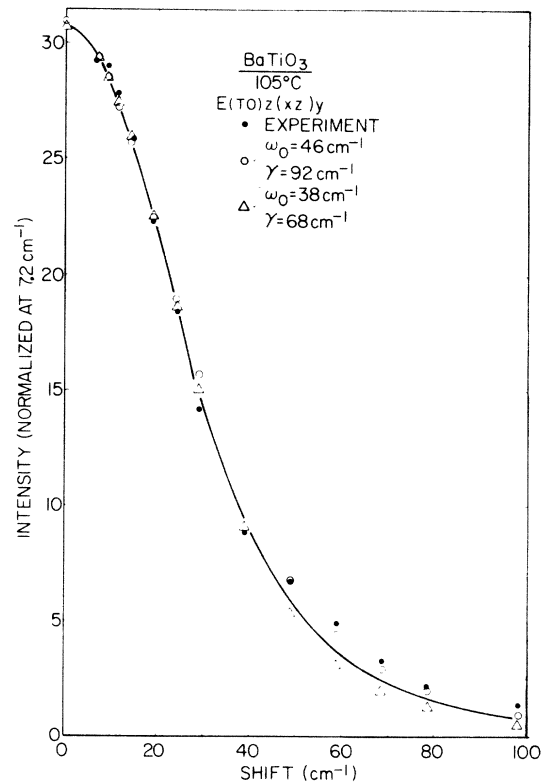


FIG. 8. Experimental and calculated results for the soft $E(\text{TO})$ mode at 105°C . The fit is discussed in the text.

lated result at 7 cm^{-1} . As indicated by the result in Fig. 8, there are a large variety of values that will fit experiment within the accuracy of the data. Naturally, if the experimental result were known to very high precision, a better comparison between theory and experiment could be made. However, there always is the very difficult experimental problem as to the shape of the background scattering (the base line). We have measured the $E(\text{TO})$ mode from room temperature to T_c and the data show that within our experimental error the shape of the mode does not change. This is in agreement with Ref. 11 as judged by the relative temperature independence of their γ/ω_0 values. Thus, from the shape alone we cannot determine the temperature dependence of the frequency or damping constant. However, a large increase in γ as T_c is approached, as shown in Fig. 6, seems highly unlikely, since a correspondingly large increase in the undamped harmonic frequency would have to occur in order to keep the shape of the Raman line independent of temperature. This would be contrary to what is expected from Fig. 5 or the dielectric behavior, to be discussed.

Next consider the total intensity of the soft $E(\text{TO})$ mode. A change of almost an order of magnitude was reported between 10 and 60°C by DiDomenico *et al.*¹¹ We observe something quite different. We have always found measurements of intensity at different temperatures a bit untrustworthy, possibly due to slight shifting of the furnace position which moves the laser beam within the sample. However, we find the intensity versus temperature of this soft $E(\text{TO})$ mode to be independent of temperature ($\approx 30\%$ might be a reasonable guess at our accuracy). The total integrated intensity of the signal should be $\propto kTP_s^2/\omega_0^2$. P_s varies²¹ from 26 to $18 \mu\text{C}/\text{cm}^2$ between 20°C and T_c , so P_s^2 varies by a factor of 2. A small variation of ω_0 , then, would be consistent with the intensity observations of our experiment and with the extrapolated behavior for BaTiO_3 in Fig. 5. The reason for the differences between the observations reported here and those reported in Ref. 11 is not known. However, it would seem that the higher-intensity results must always be correct.

Separate from the above observations, we would like to comment on the behavior of the lines at T_c . We observe that at T_c the soft $E(\text{TO})$ mode, as well as the other E modes, disappear abruptly ($\frac{1}{2}^\circ\text{C}$ steps are taken). These modes reappear, just as abruptly, as temperature is lowered. On heating, the modes disappear at 135°C and reappear, on cooling, at 131°C . This thermal hysteresis is expected for a first-order phase transition and is in agreement with measurements of the temperature dependence of the dielectric constant. The A_1 modes have also been reported¹⁴ to disap-

pear and reappear abruptly at T_c . So all the first-order Raman modes behave as expected at T_c just as has been observed¹ in PbTiO_3 .

VI. DISCUSSION

A. $0 < x < 1$ data

One of the most surprising results is that the soft $E(\text{TO})$ mode is underdamped over most of the range of x . Only very near BaTiO_3 does the mode become overdamped. The fact that this is observed in solid solutions is even more surprising. Clearly, there is something special about BaTiO_3 that causes this mode to be overdamped. From the neutron scattering results^{27,28} for BaTiO_3 , one finds that for the lowest transverse optic branch, certain directions of the wave vector \vec{q} and certain polarizations \vec{e} show well-defined phonons, except for very small q values. However, for other values of q and e the optic branch is unusually low in energy and highly damped throughout the entire Brillouin zone. Thus, in BaTiO_3 the lowest transverse optic branch is very anisotropic. This possibility was suggested by Hüller²⁹ to explain the anomalous x-ray scattering results.³⁰ On the other hand, the neutron-diffraction results³¹ for PbTiO_3 show a well-defined lowest transverse optic branch except at very small q values. It would be interesting if the energy of all the phonon branches could be observed throughout the Brillouin zone to compare with Silverman's theory²² of line broadening for these two materials.

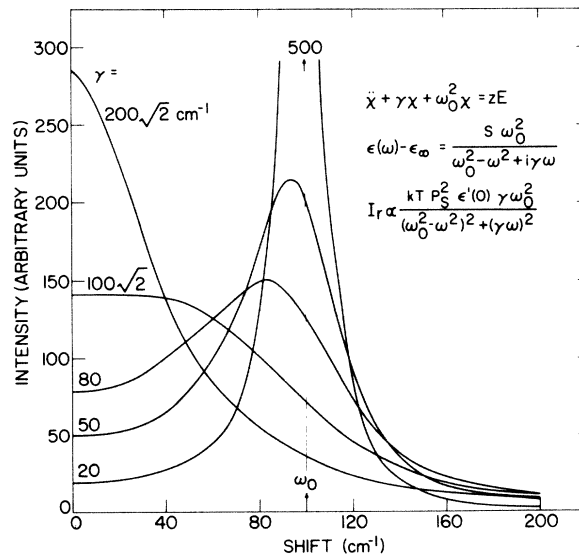


FIG. 9. Calculated Raman response, in the high-temperature limit, for a mode for various values of γ/ω_0 from an underdamped case (20/100) to an overdamped case ($2\sqrt{2}$).

The frequencies of the modes vary smoothly with x . This occurs even though phase transitions occur at low temperatures. So the restoring forces for the different modes appear to vary in a fairly smooth way with x , even through the first-order phase transitions.

B. BaTiO₃

First, we remark again that all the $3n-3$ normally expected modes in BaTiO₃ do disappear abruptly at the tetragonal to cubic phase transition. These modes reappear abruptly as the crystal is cooled and goes from a cubic to tetragonal phase. So as long as attention is focused on the $3T_{1u} + T_{2u}$ modes in O_h and the corresponding modes in the tetragonal or lower-temperature phase, the selection rules are obeyed. Of course, there are other broad bands that are observed in the Raman spectra of $x=1$ (but not for smaller x ¹³). There is a great deal of discussion about these bands³² and attempts to relate them to an order-disorder model.^{32,33} We cannot further clarify this point.

Second, the temperature dependence of the frequency of the soft $E(\text{TO})$ phonon is not as yet determined. Our data, particularly with respect to intensity, are not in agreement with earlier data.¹¹ Certainly it is possible to get frequencies and damping constants from our data that vary and are different from the earlier data.¹¹ There have been some studies of this soft $E(\text{TO})$ mode apparently under much higher signal-to-noise conditions.³⁴⁻³⁶ These results are at room temperature but would be interesting if extended to T_c .

Last, we would like to discuss the value of the zero-frequency clamped dielectric constant $\epsilon(0)$ and its determination from the modes. The Lydane-Sachs-Teller (LST) relation is²

$$\frac{\epsilon(0)}{\epsilon_\infty} = \prod_i \frac{\omega_{\text{LO}i}^2}{\omega_{\text{TO}i}^2}, \quad (3)$$

where ϵ_∞ is the square of the optic index of refraction and the product is over all three normal modes in BaTiO₃. For axial ferroelectrics this equation applies separately to the dielectric constant along the c axis (ϵ_c) or along the a axis (ϵ_a). For ϵ_c the vibrational modes transform as the A_1 -irreducible representation of the point group C_{4v} . For ϵ_a the modes transform as the E -irreducible representation. For this discussion we define ϵ_m as the value of $\epsilon(0)$ calculated from Eq. (3) via the lattice normal modes, which usually means measurements down to 30 cm⁻¹. Define ϵ_{cap} as the value of the clamped dielectric constant, measured by capacitance techniques usually in the range 10⁷–10¹⁰ Hz (i.e., below 1 cm⁻¹). In a previous paper³⁷ we have pointed out that in BaTiO₃ and other ferroelectrics, for the dielectric constants along the ferroelectric c axis, $\epsilon_{\text{cap}}/\epsilon_m > 1$ and becomes larger

as T_c is approached from below. We have discussed this in terms of dirty displacive ferroelectrics (a ferroelectric with a certain amount of disorder in the crystals).

Now consider the E modes and the dielectric constant along the a axis. From the LST relationship, $\epsilon_m = 1700$ at 30 °C is obtained.¹¹ More recent experimental values are 1500 (Ref. 35) and 1250 ± 350.³⁶ The latter value is interesting since it is determined directly from the slope of a polariton curve and is thus independent of the LST relation. The measured value of the clamped dielectric constant along the a axis is 2300.³⁸ So, there is a discrepancy along the a axis that is similar to the one along the c axis. A determination of the temperature dependence of this effect would be very interesting.

We have shown³⁹ that the clamped dielectric constant measured at microwave frequencies can be enhanced considerably by a coupling between impurities and the normal modes. For example, if an impurity, given the subscript 1, is coupled to the soft mode, subscript m , one obtains, in the range $\omega \ll \omega_m$,

$$\epsilon = \epsilon_\infty + \epsilon_m + \frac{\Omega_1^2 [\frac{1}{3}(\epsilon_m + 2)]^2}{\omega_1^2 - \frac{1}{3}\Omega_1^2 [\frac{1}{3}(\epsilon_m + 2)] - \omega^2}, \quad (4)$$

where $\Omega_1^2 = 4\pi n_1 e_1^2 / m_1$. If the coupling were zero, the square-bracket terms would be replaced by 1, and the equation would be just what is expected from an additional oscillator, an impurity in this case, contributing to ϵ . However, for ferroelectrics where ϵ_m , given by the LST relation, can be very large, the effect of impurities can be considerably enhanced. For example, for BaTiO₃ along the c axis, ϵ_m varies with temperature from about¹⁴ 31 to 48; taking the impurity to have the mass of a titanium atom with one electronic charge and a frequency of 5 cm⁻¹ using Eq. (4), the density of such impurities would have to be 4.25 × 10¹⁸/cm³ to explain the observed temperature dependence of ϵ_{cap} . This is not excessive. For the a axis, where $\epsilon_{\text{cap}} = 2300$ and $\epsilon_m \approx 1500$, and using the same impurity as above, about 10⁵ fewer impurities are required to explain the data. Such an impurity content is quite likely in BaTiO₃. Questions certainly arise: How are the impurities really coupled to the lattice modes, and what is their effective charge and mass? However, it does seem that such a simple model can explain some of the discrepancies between ϵ_{cap} and ϵ_m .

ACKNOWLEDGMENTS

It is a pleasure to thank Dr. B. A. Scott for his interest in this work and for preparing the crystals and ceramics used here. F. Dacol's

technical assistance throughout all phases of the measurements is also gratefully acknowledged.

Useful discussions with Dr. B. D. Silverman and Dr. Y. Yamada are also gratefully acknowledged.

- [†]Partially supported by the Army Research Office, Durham, N.C.
- ¹G. Burns and B. A. Scott, *Phys. Rev. B* **7**, 3088 (1973), hereafter referred to as I. See also G. Burns and B. A. Scott, *Phys. Rev. Lett.* **25**, 162 (1970).
- ²(a) F. Jona and G. Shirane, *Ferroelectric Crystals* (Macmillan, New York, 1962); (b) E. Fattuzzo and W. J. Merz, *Ferroelectricity* (Wiley, New York, 1967); (c) W. Kaenzig, in *Solid State Physics*, edited by F. Seitz and D. Turnbull (Academic, New York, 1957), Vol. 4, pp. 1-197.
- ³W. Cochran, *Phys. Rev. Lett.* **3**, 412 (1959); *Adv. Phys.* **9**, 387 (1960); **10**, 401 (1961).
- ⁴W. G. Spitzer, R. C. Miller, D. A. Kleinman, and L. E. Howarth, *Phys. Rev.* **126**, 1710 (1962).
- ⁵T. M. Ballantyne, *Phys. Rev.* **136**, A429 (1964).
- ⁶A. S. Barker, Jr., *Phys. Rev.* **145**, 931 (1966).
- ⁷M. DiDomenico, Jr., S. P. S. Porto, and S. H. Wemple, *Phys. Rev. Lett.* **19**, 855 (1967).
- ⁸G. Burns and B. A. Scott, *Phys. Rev. Lett.* **25**, 1191 (1970); G. Burns, *Mater. Res. Bull.* **6**, 923 (1971).
- ⁹J. L. Parsons and L. Rimai, *Solid State Commun.* **5**, 423 (1967); L. Rimai, J. L. Parsons, J. T. Hickmott, and T. Nakamura, *Phys. Rev.* **168**, 623 (1968).
- ¹⁰A. Pinczuk, W. T. Taylor, E. Brustein, and I. Lefkowitz, *Solid State Commun.* **5**, 429 (1967).
- ¹¹M. DiDomenico, Jr., S. H. Wemple, S. P. S. Porto, and R. P. Bauman, *Phys. Rev.* **174**, 522 (1968).
- ¹²A. Pinczuk, E. Burstein, and S. Ushioda, *Solid State Commun.* **1**, 139 (1969).
- ¹³G. Burns and B. A. Scott, *Solid State Commun.* **9**, 813 (1971).
- ¹⁴G. Burns, *Phys. Lett. A* **43**, 271 (1973).
- ¹⁵J. P. Remeika, *J. Am. Chem. Soc.* **76**, 940 (1954).
- ¹⁶G. Shirane and K. Suzuki, *J. Phys. Soc. Jap.* **6**, 274 (1951).
- ¹⁷H. F. Kay and P. Vousden, *Philos. Mag.* **40**, 1019 (1949).
- ¹⁸B. Lewis and E. A. D. White, *Acta Crystallogr.* **8**, 849 (1955).
- ¹⁹S. Nomura and S. Sawada, *J. Phys. Soc. Jap.* **6**, 36 (1951).
- ²⁰J. P. Remeika and A. M. Glass, *Mater. Res. Bull.* **5**, 37 (1970).
- ²¹W. J. Merz, *Phys. Rev.* **91**, 513 (1953).
- ²²B. D. Silverman, *Solid State Commun.* **10**, 311 (1972).
- ²³T. G. Davis, *Phys. Rev. B* **5**, 2530 (1972).
- ²⁴Y. S. Bobovich and E. V. Bursian, *Opt. Spektrosk.* **11**, 131 (1961) [*Opt. Spectrosc.* **11**, 69 (1961)].
- ²⁵S. Ihegami, *J. Phys. Soc. Jap.* **19**, 46 (1964).
- ²⁶C. H. Perry and D. B. Hall, *Phys. Rev. Lett.* **15**, 700 (1965).
- ²⁷G. Shirane, J. D. Axe, and J. Harada, *Phys. Rev. B* **2**, 3651 (1970).
- ²⁸J. Harada, J. D. Axe and G. Shirane, *Phys. Rev. B* **4**, 155 (1971).
- ²⁹A. Hüller, *Z. Phys.* **220**, 145 (1969).
- ³⁰R. Comes, M. Lambert, and A. Guinier, *Solid State Commun.* **6**, 715 (1968); **7**, 305 (1969).
- ³¹G. Shirane, J. D. Axe, J. Harada, and J. P. Remeika, *Phys. Rev. B* **2**, 155 (1970).
- ³²M. P. Fontana and M. Lambert, *Solid State Commun.* **10**, 1 (1972); A. M. Quittet and M. Lambert, *Solid State Commun.* **12**, 1053 (1973).
- ³³G. A. Barbosa, A. Chaves, and S. P. S. Porto, *Solid State Commun.* **11**, 1053 (1972).
- ³⁴P. A. Fleury and P. D. Lazay, *Phys. Rev. Lett.* **26**, 1331 (1971).
- ³⁵L. Loughman, L. W. Davis, and T. Nakamura, *Phys. Rev. B* **6**, 3322 (1972).
- ³⁶D. Heiman and S. Ushioda, *Phys. Rev. B* **9**, 2122 (1974).
- ³⁷G. Burns and B. A. Scott, *Solid State Commun.* **13**, 417 (1973).
- ³⁸S. H. Wemple, M. DiDomenico, Jr., and I. Camlibe, *J. Phys. Chem. Solids* **29**, 1797 (1968).
- ³⁹G. Burns and E. Burstein, *Ferroelectrics* **7** (to be published).